Original Research

Rictor is involved in *Ctnnd2* deletion-induced impairment of spatial learning and memory but not autism-like behaviors

Xiaoya Wang[1,2,3], Man Xu[1,2], Qingbao Xu[4], Feng Yang[5], Hui Tang[3], Chuan Shao[3], Luyi Wang[1,2], Yan Wang[1,2], Jing Deng[1,2], Shali Wang[1,2,*]

[1]*Cerebrovascular Disease Laboratory, Institute of Neuroscience, Chongqing Medical University, 400016 Chongqing, China,* [2]*Department of Physiology, School of Basic Medical Sciences, Chongqing Medical University, 400016 Chongqing, China,* [3]*Department of Neurosurgery, Nanchong Central Hospital, The Second Clinical Medical College, North Sichuan Medical College, 637100 Nanchong, Sichuan, China,* [4]*Department of Operating room, Nanchong Central Hospital, The Second Clinical Medical College, North Sichuan Medical College, 637100 Nanchong, Sichuan, China,* [5]*China National Clinical Research Center for Neurological Diseases, Beijing Tiantan Hospital, Capital Medical University, 100070 Beijing, China*

TABLE OF CONTENTS

1. Abstract

Background: The *CTNND2* gene which encodes a δ-catenin protein (CTNND2) is associated with multiple severe neurological disorders. However, the specific role of *CTNND2* in spatial cognition and related mechanisms remains obscure. **Methods**: In this study, we generated a new line of *Ctnnd2*-Knock out (KO) mice with its exon2 deleted, and then characterized their behavioral phenotypes and explore the Biological mechanism. **Results**: *Ctnnd2*-KO mice were with typical autism-like behaviors as evidenced by reduced social interaction in three-chamber sociability test, more frequent stereotypic behaviors (self-grooming), and deficits in spatial learning and

Submitted: 2 July 2021 Revised: 25 July 2021 Accepted: 11 August 2021 Published: 30 August 2021

memory tested by the Morris water maze. Furthermore, the expression of Rictor protein, a core component of the mTORC2 complex, was significantly decreased in the hippocampus of mutant mice. ShRNA-induced knockdown of Rictor protein in the hippocampus of both *Ctnnd2*-KO mice and wild-type mice exacerbated spatial learning and memory deficits but did not affect their autism-like behaviors. Mechanistically, the hippocampal CA1 neurons of *Ctnnd2*-KO mice showed decreased actin polymerization, postsynaptic spine density. Down-regulation of Rictor resulted in altered expression of post-synaptic proteins such as GluR1 and ELKS, but not presynaptic protein Synapsin1, implying abnormal synaptic changes in KO mice. **Conclusion**: The *CTNND2* gene is involved in spatial learning and memory *via* Rictor-mediated actin polymerization and synaptic plasticity. Our study provides a novel insight into the role and mechanisms of the *Ctnnd2* gene in cognition at the molecular and synaptic levels.

Highlights

1. *Ctnnd2*$^{-/-}$ mice exhibited autism-like behaviors and impaired spatial learning and memory.
2. Rictor was involved in the regulation of *Ctnnd2*-associated spatial cognition but not autism-like behaviors.
3. Rictor played a crucial role in spatial learning and memory by modulating postsynaptic changes in hippocampal neurons of *Ctnnd2*$^{-/-}$ mice.

2. Introduction

CTNND2 gene that encodes for a δ-catenin protein, contains 23 exons, spans at least 640 kb, and maps in 5p15.2 region of human chromosome. Clinical studies revealed that *CTNND2* variations have been implicated in multiple neurological disorders, such as Cri-du-chat syndrome, epilepsy, bipolar disorder, and schizophrenia [1]. *CTNND2* was also considered as a candidate gene for intellectual disability [2]. Loss-of-function mutations in *CTNND2* were closely related to a severe familial form of autism spectrum disorder (ASD) [3]. As known, these neurological diseases shared multiple common symptoms including deficits in cognition especially learning and memory. Although specific genes in the hippocampus that are associated with learning and long-term memory had been reported before, whether *CTNND2* is associated with cognitive performance is unknown [4], Previous studies had shown that *CTNND2* was essential for proper neuronal migration [3], dendritic morphogenesis and synapse maturation [5] which have been suggested the basis of learning and memory. *Ctnnd2* deficiency caused abnormal synaptic plasticity in mice [5]. The δ-catenin, *CTNND2* gene-encoded protein, targeted to dendrite spines via interacting with N-terminus of Shank3 [6], an upstream node of the phosphatidylinositol 3-kinase (PI3K)/atypical kinase (AKT) pathway and had great effects on mammalian target of rapamycin (mTOR) signaling [7]. Whether the *CTNND2* gene or δ-catenin protein modulate learning and memory via mTOR signaling remains unknown.

An important cellular signaling node (mTOR signaling) is mediated by two structurally and functionally distinct complexes, mTORC1 and mTORC2 [8]. The later complex, mTORC2 is a multimeric kinase [9, 10], and contains various key components, Recent studies have demonstrated that mTORC2 could promote cellular survival by activating AKT phosphorylation at Ser473 [11] and regulate the cytoskeletal dynamics and structural changes at synapses, which is essential for cognitive function [12, 13]. Rictor, a core component of mTORC2, specifically regulates actin cytoskeletal dynamics to control spine morphogenesis through dynamic transitions between monomeric G-actin and F-actin, including the size of postsynaptic spines at glutamatergic synapses [14]. Rictor-knockout mice exhibit decreased actin polymerization [12]. As a consequence, aberrant Rictor-mediated actin polymerization contributes to age-related memory loss [15], which is highly associated with abnormal hippocampal synaptic plasticity. However, whether *CTNND2* gene or δ-catenin protein play a role in regulating learning and memory via Rictor has not been elucidated.

Synaptic plasticity is necessary for information encoding and storage and constitutes the basis of cognitive activities within the brain [16, 17]. A series of studies have indicated that structural changes in the hippocampus are critical for higherorder cognition and behavior [18, 19]. In hippocampal neurons, dendrites are the major sites for synaptic input and integration, where the spines are the key apparatus for neurotransmission, and its morphology is altered by stimuli [20, 22]. Indeed, spine morphology is largely dependent on actin cytoskeleton dynamics under the control of Rictor [14]. Thus, knockdown of Rictor reduced actin polymerization and attenuated the alterations in spine head size, as well as the number of mature mushroom spines in the dorsomedial striatum of mice [23]. Moreover, Rictor deficiency also affects the size, morphology, and function of neurons [24]. Based on these evidence, Rictor may largely be involved in the pathogenesis of *CTNND2* deficiency-mediated learning and memory deficiency.

Thus, in this study, we generated *Ctnnd2*-knockout (KO) mice and characterized their autism-like behaviors, spatial cognition, and the expression of Rictor protein in the hippocampus. We further performed virus-mediated Rictor knockdown and observed the changes in behavioral phenotypes of *Ctnnd2*-KO mice. To uncover the mechanism of the *CTNND2* gene participating in the modulation of learning and memory, several key molecules in the mTOR signaling pathway and neural synaptic structures and components were measured.

3. Methods

3.1 Animal genotyping and treatments

All animal experiments were conducted under the National Institutes of Health Guide for the Care and Use of Laboratory Animals. C57BL/6 mice were obtained from the Experimental Animal Center of Chongqing Medical University. *Ctnnd2* KO (*Ctnnd2*$^{-/-}$) mice in a C57BL/6 background were generated by CRISPR/Cas-mediated genome engineering, in collaboration with Nanjing Institute of Biomedicine, Nanjing University. Briefly, both Cas9 mRNA and sgRNA were microinjected into the zygotes, where sgRNA directed Cas9 endonuclease to cleave within intron 1-2 and intron 2-3 of mouse *Ctnnd2* gene, yielding a double-strand break (DSB). Such breaks were then repaired by non-homologous end joining and proposed to result in disruption of *Ctnnd2* gene expression *in vivo*. We bred the homozygous mutant mice from heterozygotes and their ups were genotyped by PCR as usual. For genotyping, mouse tail DNA fragments were amplified by PCR using the following primers: 5′-TTCTGTATTTCACAGTACCAAC-3′/5′-AACTCATCATAAGAAACACCTG-3′, and 5′-ACAGAATTATATCACACTTGTCC-3′/5′-ACTGTCACCCTACTTTAGTGTTA-3′.

All mice were housed at (25 ± 3 °C) and relative humidity (55% ± 5%) under a 12 h/12 h light/dark cycle. The corresponding adenovirus was conducted on experimental male mice on a postnatal day (PND) 21 and behavior tests on PND49. Mice were then sacrificed for further analyses. No animals were excluded from the analysis.

3.2 Virus vector construction

The adeno-associated virus (AAV)-based Rictor RNA interference vector pAKD-CMV-bGlobin-GPR-H1-shRNA (AAV-Rictor) were constructed by Obio Technology, Shanghai China, containing the target sequences (GCCAGTAAGATGGGAATCA, sense; TGATTCCCATCTTACTGGC, antisense). The verification of the inhibitory efficiency on Rictor expression was conducted 4 weeks later after the AAV injection.

3.3 Surgery and stereotaxic injection

Mice were anesthetized with an intraperitoneal injection of sodium pentobarbital (100 mg/kg, *i.p.*) and then fixed in a stereotaxic frame (Stoelting Instruments, Wood Dale, IL, USA). AAV (3.61 × 10^{12} TU/mL, 0.5 μL total volume per side) was injected bilaterally into the dorsal hippocampus (AP: –1.7 mm, ML: ± 1.3 mm, DV: –1.0 mm) over 5 min (injection rate of 0.1 μL per min). The syringe was maintained *in situ* for at least 5 min after every injection, to limit reflux along the injection tracks. Behavioral tests were conducted 4 weeks later.

3.4 Behavioral tests

3.4.1 Three-chamber test

A three-chamber box (length × width × height, 120 cm × 20 cm × 22 cm) was used to assess social interaction and novelty preference behavior of animals. The left and right compartments were equipped with small empty cages. Each mouse was habituated to the three chambers for 10 min before the test. In the first period of the test, a same-sex stranger mouse (stranger 1) was placed in one of these two cages, while the test mouse was placed in the middle chamber. In phase 1, movements of the test mouse were recorded for 10 min to determine time spent on exploring and interacting with stranger 1 and with the empty cage (object), as an index of sociability. 10 min later, a new stranger mouse was placed in the other cage (stranger 2), and the test mouse was placed in the middle chamber. Again, movements were recorded for 10 min to assess the time exploring and interacting with strangers 1 and 2 as an index of social novelty preference. Analyses were performed in a manner with blinded treatment assignments using EthoVision XT 11.5 (Noldus, Netherlands). The chambers were cleaned with 70% ethanol between trials.

3.4.2 Open field test

The open field was a 40 cm × 40 cm open arena, with 30 cm high walls, and the floor was divided into 16 squares of the equal area by a grid of black lines. The animals were acclimated to the testing room for 1 h and then to the open field for 10 min before the 10-min test session. The time of grooming behaviors, the number of squares that animals passed through (grid crossing), frequency of straight upward movements (vertical rearing), and the number of climbing episodes were recorded. Analyses were performed in a manner with blinded treatment assignments using EthoVision XT 11.5 (Noldus, Netherlands). The open field was thoroughly cleaned with 70% alcohol between trials.

3.4.3 Morris water maze test

The classic Morris water maze test was used to evaluate spatial learning and memory. In the place navigation, the mice firstly completed a 5-day training. In each trial, the mouse was required to locate and mount a submerged platform (10 cm × 10 cm) located within a circular black pool (diameter 120 cm) filled with white opaque water (25 ± 1 °C). If the mouse did not locate the platform within 60 s, it was gently guided to it and allowed to stay for 15 s. During this phase, the platform location was kept constant while the starting point varied among the four quadrants of the pool (L: left quadrant; R: right quadrant; T: target quadrant; O: opposite quadrant). In the spatial probe test on day 6, the platform was removed, and the animal was allowed to swim freely for 60 s. For analysis, the swimming time in the target quadrant and distance in the quadrant in which the platform had previously been located

and the platform-crossing times were recorded by a tracking system connected to an image analyzer (HVS Image, Hampton, UK) in a double-blind manner.

3.5 Golgi-Cox staining

Golgi-Cox staining was performed to examine the neuronal spine density of the hippocampus using an FD Rapid Golgi Stain Kit (PK401; FD Neuro-Technologies, Columbia, USA), according to the manufacturer's instructions. After anesthetized, the brains of the mice were rapidly removed. After rising in distilled water, brains were immersed in a 1:1 (v/v) mixture of Solutions A and B for 2 days, and then kept at room temperature for 2 weeks. Brains were then immersed in Solution C and stored at 4 °C for another 3 days. After that, brains were cut into 100-μm thick coronal sections, which were mounted on gelatin-coated slides and dried naturally. Then slides were stained with a mixture of Solution D, Solution E, and distilled water (1:1:2) for 10 min. After another wash with distilled water, the slides were dehydrated by 4 cycles in gradient ethanol (50%, 75%, 90%, 100%, and 100%, each for 4 min) and then cleared with xylene. The hippocampal areas were imaged using an Olympus microscope system. The number of dendritic spines along the secondary branches of CA1 pyramidal neuron dendrites were counted from 6 cells per hippocampus and the mean number for each 10-μm dendritic length measured in a double-blinded manner by ImageJ software (1.6.0, National Institutes of Health, New York, USA).

3.6 Electron microscopy analysis

Transmission electron microscopy (TEM) was used to evaluate the density of spine synapses and the thickness of postsynaptic density (PSD) within the mouse hippocampus of each group. Briefly, mice were deeply anesthetized, and both hippocampi isolated. The hippocampi were transferred into 2.5% glutaraldehyde and kept at 4 °C for 24 h, cut into slices, and fixed in glutaraldehyde for further 3 days. The slices were then washed in PBS, fixed in 1% osmium tetroxide, stained with an aqueous solution of 2% uranyl acetate, dehydrated in a gradient of alcohol and acetone, embedded in an embedding medium, incubated in an oven, and cut into ultrathin sections. The sections were stained with 4% uranyl acetate and citrate and examined under a transmission electron microscope (JEM-1400 Plus, JEOL, Japan) at 40,000× and 100,000× magnification. Both the synaptic density and the PSD thickness were analyzed using Image-Pro Plus 6.0 (Media Cybernetics Inc.). The number of synapses *per* unit volume of tissue (Nv) was calculated from the number of synapses *per* unit of area (Na) according to the formula $Nv = 8ENa / \pi^2$ (where E is the mean of the reciprocals of the observed PSD lengths for each synaptic profile category), as described previously [25].

3.7 Western blotting

Western blot analyses were performed to examine the expression of targeted proteins within the hippocampus. Hippocampi were isolated rapidly and then lysed in RIPA buffer (P0013B; Beyotime, Shanghai, China) with a 15% protease inhibitor cocktail (4693116001, Roche, Basel, Switzerland). Protein concentration was measured with an Enhanced BCA assay kit (P0012, Beyotime), according to the manufacturer's instructions. Extracted proteins were then transferred to PVDF membranes (Millipore, Billerica, MA, USA). Membranes were blocked by incubation for 1.5 h at room temperature in freshly prepared TBST containing 5% skim milk, and then incubated with the indicated primary antibodies at 4 °C overnight. Immunoblotted membranes were washed with TBST, and incubated with horseradish peroxidase (HRP)-conjugated anti-goat, anti-rabbit, and anti-mouse secondary antibodies for 1 h at 37 °C, respectively. The protein bands were visualized with Western Lighting-ECL and quantified using ImageJ (1.6.0, National Institutes of Health, New York, USA). All experiments were repeated at least three times on independently prepared lysates from different mice.

The F-actin/G-actin ratio analysis was according to the previous studies [26]. Briefly, the hippocampi were homogenized in cold lysis buffer and centrifuged at 15,000g for 30 min to obtain soluble actin (G-actin) in the supernatant. The pellet was re-suspended in the same volume of lysis buffer and incubated at 4 °C for 1 h to depolymerize the insoluble F-actin. This suspension was then centrifuged at 15,000 rpm for 30 min to obtain F-actin in the supernatant. Equal amounts of G-actin and F-actin were loaded onto gels and analyzed by western blot.

The primary antibodies and dilutions were as follows: rabbit anti-Rictor (1:1000, 2140, Cell Signaling Technology, Danvers, MA, USA), rabbit anti-phospho-AKTSer473 (1:1000, 9271, Cell Signaling), rabbit anti-AKT (1:1000, 9272, Cell Signaling) rabbit anti-actin (1:1000, GTX61452, Gentex, Zeeland, MI, USA), rabbit anti-cofilin (1:1000, 3312, Cell Signaling), rabbit anti-profilin-1 (1:1000, GTX63456, Gentex), rabbit anti-GluR1 (1:1000, 2452486, Millipore, Burlington, MA, USA), rabbit anti-synapsin 1 (1:30000, AB1543, Millipore), rabbit anti-ELKS (1:5000, 180507, Abcam, Cambridge, UK), and mouse anti-β-actin (1:2000, AA128, Beyotime Biotech) as the loading control. The secondary antibodies included HRP-conjugated goat anti-rabbit lgG and HRP-conjugated goat anti-mouse IgG (1:2000, ZB-2301 and ZB-2305, Zhongshan Biotech).

3.8 Statistical analysis

All graphs show the means ± S.E.M. from at least 3 separate experiments. Statistical analyses were performed using SPSS 21.0 (IBM, Armonk, NY, USA). In experiments with two treatment groups, means were compared by two-tailed independent-samples Student's *t*-test. Multiple

groups mean with normal distributions and equality of variance were compared by one- or two-way ANOVA with *post hoc* Tukey's tests for multiple pair-wise comparisons. Morris water maze test data were analyzed by two-way repeated mixed measures ANOVA with *post hoc* Tukey's tests. Values of $p < 0.05$ were considered to be significant.

4. Results

4.1 *Ctnnd2*$^{-/-}$ mice exhibited autism-like behaviors and deficits in spatial learning and memory

Using a CRISPR/Cas9-mediated gene-targeting strategy, we generated mutant mice with exon 2 deleted within the endogenous murine *Ctnnd2* gene (Fig. 1A). Heterozygous mice were used to produce the homozygotes and their wild-type (WT) control littermates. Genotyping was applied to identify the mutant mice by two different pairs of primers, yielding a 1074 bp/421 bp fragment pattern for wild-type and 459 bp/- for *Ctnnd2*$^{-/-}$ mice (Fig. 1B). In three-chamber sociability tests, the total entries showed a no difference between WT and *Ctnnd2*$^{-/-}$ mice (Fig. 1D,G) but *Ctnnd2*$^{-/-}$ mice spent less time interacting with stranger 1 ($p < 0.05$) and more time staying in the center chamber ($p < 0.01$) in social interaction test, compared with the WT mice (Fig. 1E). Meanwhile, *Ctnnd2*$^{-/-}$ mice spent more time staying in the center chamber ($p < 0.05$) and less time interacting with the stranger 2 ($p < 0.05$) in the novelty preference test (Fig. 1H). In the open field test, *Ctnnd2*$^{-/-}$ mice showed stereotypic and repetitive behaviors as we observed more grooming frequency of them than the WT ones ($p < 0.001$; Fig. 1J). Moreover, *Ctnnd2*$^{-/-}$ mice exhibited anxiety-like behaviors, as evidence by the reduced number of center grid crossings ($p < 0.01$; Fig. 1K) and vertical ($p < 0.01$; Fig. 1L). Additionally, *Ctnnd2*$^{-/-}$ mice showed abnormal exploratory behaviors, as evidenced by decreased numbers in climbing ($p < 0.01$; Fig. 1M). The total cross grid number showed no difference between WT and *Ctnnd2*$^{-/-}$ mice (Fig. 1N). These data suggest that *Ctnnd2*$^{-/-}$ mice showed decreased social interaction and novelty preference, stereotypic and anxiety-like behaviors, decreased exploratory behaviors.

Next, we used the Morris water maze (MWM) to evaluate the hippocampus-dependent spatial learning and memory. In the learning phase, a two-way repeated-measures ANOVA revealed that both day ($F_{(4,32)} = 23.537$, $p < 0.01$) and group ($F_{(1,14)} = 9.425$, $p < 0.01$) could affect the escape latencies, but no detectable day × group interaction ($F_{(4,32)} = 1.371$, $p > 0.05$). A *post hoc* analysis showed that there was significance between WT and *Ctnnd2*$^{-/-}$ mice ($p > 0.05$ for Day 1 and Day 2, $p < 0.05$ for Day 3, Day 4, Day 5; Fig. 2A). *Ctnnd2*$^{-/-}$ mice spent significantly more time finding the hidden platform than the WT mice ($p < 0.05$) from day 3 to day 5 ($p < 0.05$, Fig. 2A,J). The swim speed showed no difference during the learning stage (Fig. 2B). For the memory test on day 6, we observed a representative swimming pathway (Fig. 2D) and quantified the time spent in each quadrant. We then found that *Ctnnd2*$^{-/-}$ mice crossed the platform less often ($p < 0.05$; Fig. 2C) and spent less time in the target quadrant ($p < 0.05$; Fig. 2E). No significant differences between WT and *Ctnnd2*$^{-/-}$ mice in swim speed and movement distance (Fig. 2F,G). Collectively, these data suggest that spatial learning and memory are impaired in *Ctnnd2*$^{-/-}$ mice.

4.2 Rictor knockdown affected spatial learning and memory but not autism-like behaviors in *Ctnnd2*$^{-/-}$ mice

As Rictor plays an important role in synapse development and synaptic plasticity in the hippocampus, we firstly explored the expression levels of Rictor protein in the hippocampus at different developing stages, using both WT and mutant mice. As shown in Fig. 3, hippocampal Rictor expression was gradually decreased with age and keep stable from post-natal days (PND) 21. Of note, Rictor protein levels in *Ctnnd2*$^{-/-}$ mice were significantly lower than that in WT mice ($p < 0.05$; Fig. 3A,B).

Given the significant changes in Rictor expression, we further conducted AAV-mediated Rictor knockdown induced by specific shRNA (Fig. 3D), with high efficiency (Fig. 3E). The expression of hippocampal Rictor was significantly downregulated ($p < 0.05$) after injection of virus carrying specific shRNA, both in WT and mutant mice (Fig. 3F). There was no significant difference between sham group and vector group (Fig. 3E). Western blotting confirmed decreased hippocampal Rictor expression in *Ctnnd2*$^{-/-}$ mice ($p < 0.05$, KO + Vector vs WT + Vector) and further reduction in *Ctnnd2*$^{-/-}$ mice receiving ShRictor-virus infection ($p < 0.01$, KO + ShRictor vs KO + Vector; Fig. 3F). In Morris water maze test, a two-way repeated measures ANOVA revealed that both day ($F_{(4,28)} = 15.64$, $p < 0.01$) and group ($F_{(3,21)} = 7.438$, $p < 0.01$) could affect the escape latencies, but no detectable day ×x group interaction ($F_{(12,84)} = 1.218$, $p > 0.05$). One-way ANOVA showed that there were significance among WT + Vector, WT + ShRictor, WT + Vector and KO + ShRictor ($p > 0.05$, WT + Vector vs WT + ShRictor for Day 1 and Day 2, $p < 0.05$ for Day 3, Day 4, Day 5; $p > 0.05$, WT + Vector vs KO + Vector for Day 1 and Day 2, $p < 0.05$ for Day 3, Day 4, Day 5; $p > 0.05$, KO + Vector vs KO + ShRictor for Day 1 and Day 2, $p < 0.05$ for Day 3, Day 4, Day 5; Fig. 4A). The *Ctnnd2*$^{-/-}$ mutant mice needed much increased time to find the hidden platform after Rictor knockdown ($p < 0.05$; Fig. 4A). The escape latency was also delayed in both WT and *Ctnnd2*$^{-/-}$ mice after Rictor knockdown ($p < 0.05$, WT + ShRictor vs WT + Vector; $p < 0.05$, KO + ShRictor vs KO + Vector, Fig. 4A). The swim speed showed no different during learning stage both day ($F_{(4,28)} = 0.1562$, $p > 0.05$) and group ($F_{(3,21)} = 0.1780$, $p > 0.05$) and day × group interaction ($F_{(12,84)} = 0.07183$, p

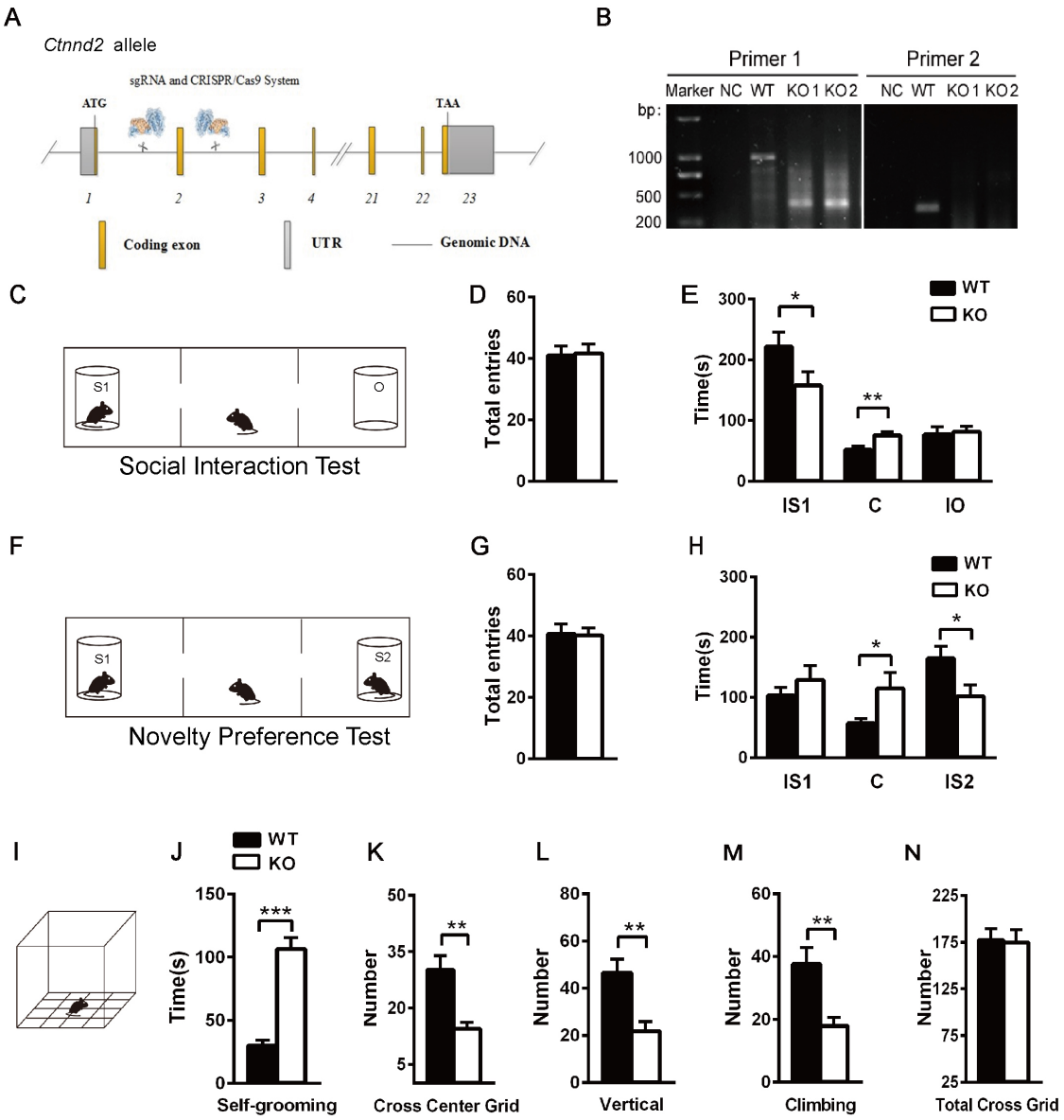

Fig. 1. Autism-like behavioral phenotypes of *Ctnnd2*$^{-/-}$ mice. (A) The strategy of generation of *Ctnnd2* mutant mice. Both Cas9 mRNA and sgRNA were co-injected into mouse zygotes; the sgRNA directed Cas9 nuclease to cleavage the exon 2 of mouse *Ctnnd2* gene and thus resulted in disruption of *CTNND2* protein. (B) Genotyping results of the mutant mice and their WT control littermates. (C–H) Three chamber test of *Ctnnd2*-mutant mice. Left panel, schematic presentation (C, F); middle panel, statistical analysis of the total entries in the social interaction test (D) and novelty preference (G), respectively; right panel, the time spent in each test (E, H). S1, stranger mouse 1; IS1, interaction with stranger mouse 1; C, center chamber; O, object; IO, interaction with the object; S2, stranger mouse 2; IS2, interaction with stranger mouse 2. (I–N) Open-field test of the mice. I, schematic presentation of the test; grooming time (J), number of center grid crossing (K), frequency of vertical rearing (L), and climbing times (M) were measured and analyzed in the open-field test. Statistical analysis was performed using a *t*-test. $n = 8$ mice per group for a behavioral test. Data are the means ± SEM. *, $p < 0.05$; **, $p < 0.01$; ***, $p < 0.001$.

> 0.05) (Fig. 4B). *Ctnnd2*$^{-/-}$ mice with shRictor-mediated knockdown made significantly fewer passes over the former platform location (Fig. 4C) and spent less time in the target quadrant (Fig. 4D). Certainly, we found no significant differences in travel distance within the target quadrant among groups (Fig. 4E). The above results indicated that virus-mediated Rictor knockdown deteriorated the impairment in learning and memory in *Ctnnd2*$^{-/-}$ mice.

We also examined whether ShRictor could affect autism-like behaviors of mutant mice in our experiments. However, when comparing these mice in the three-chamber test, the open field test, we found no significant difference between *Ctnnd2*$^{-/-}$ mice with or without virus-mediated shRNA knockdown of Rictor, as well as that between WT mice (Fig. 5). These results indicated that *Ctnnd2*$^{-/-}$ mice showed no changes in autism-like behavior after ShRictor-

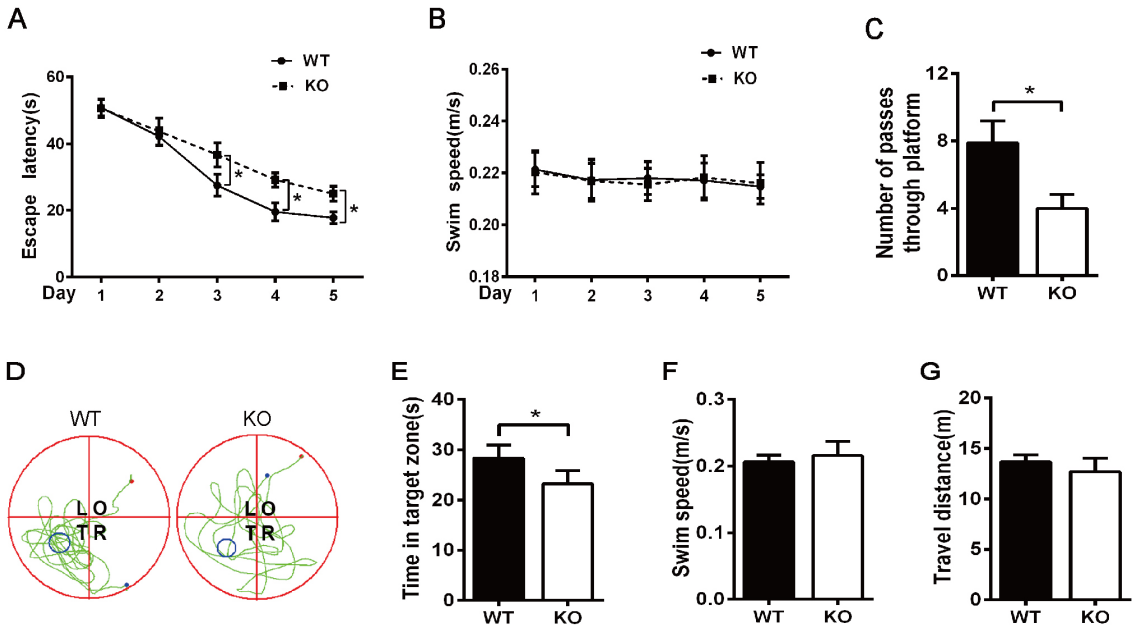

Fig. 2. The spatial learning and memory impairment in *Ctnnd2*$^{-/-}$ mice. (A–G) Morris water maze test of the mice. Escape latency time to find the submerged platform and swim speed was observed from day 1 to day 5 of the learning phase (A, B). Statistical analysis was performed using two-way ANOVA followed by *post hoc* Tukey's test for multiple comparisons. Representative swimming traces were shown for probe test (D): T, target quadrant; L, left of target quadrant; R, right of target quadrant; O, opposite of target quadrant. The number of platform crossings (C) and time in the target zone (E) during the probe trial on day 6 were analyzed to evaluate the mice's spatial memory. Two genotypes in swim speed (F) and travel distance (G) during the memory test. Statistical analysis was performed using a *t*-test. $n = 8$ mice per group. Data are the means ± SEM. *, $p < 0.05$.

induced knockdown, suggesting that Rictor was not involved in δ-catenin-related regulating of autism-like behaviors.

4.3 Rictor knockdown affects actin dynamics in *Ctnnd2*$^{-/-}$ neurons

With less expression of Rictor in the hippocampus after shRNA-mediated knockdown both in *Ctnnd2*$^{-/-}$ mice and WT controls (Fig. 3E,F), one of its downstream Akt protein showed dramatically reduced phosphorylation at Ser473 in mutant mice ($p < 0.05$, KO + Vector vs WT + Vector) and a further decrease after ShRictor-virus infection ($p < 0.05$, KO + ShRictor vs KO + Vector), as revealed by Western blotting experiments (Fig. 6A). Importantly, the F-actin/G-actin ratio, an important biomarker of actin cytoskeleton polymerization in neurons, was greatly reduced in both *Ctnnd2*$^{-/-}$ mice ($p < 0.05$, KO + Vector vs WT + Vector) and *Ctnnd2*$^{-/-}$ mice with ShRictor ($p < 0.05$, KO + ShRictor vs KO + Vector) (Fig. 6B). Moreover, the expression of Profilin-1, a polymerization regulator, was also significantly reduced in *Ctnnd2*$^{-/-}$ mice ($p < 0.05$, KO + Vector vs WT + Vector), that was exaggerated by ShRictor-mediated knockdown in the mutant mice ($p < 0.05$, KO + ShRictor vs KO + Vector) (Fig. 6C). However, the expression of cofilin protein, a de-polymerization regulator, showed no significant changes among all groups ($p > 0.05$; Fig. 6D). Taken together, mTORC2/Akt signaling is thus implicated in the regulation of Rictor-induced actin dynamics in hippocampal neurons of *Ctnnd2*$^{-/-}$ mice, implying a neuronal basis for their behavioral changes.

4.4 Rictor knockdown affects hippocampal synaptic morphology and function of *Ctnnd2*$^{-/-}$ mice

As actin dynamics is key to neuronal dendritogenesis, we subsequently detect the dendritic spine density using classic Golgi-like staining (Fig. 7A, left panel). We found that mutant mice exhibited less spine density than the WT littermates ($p < 0.05$), and this reduction was further exacerbated by ShRictor in *Ctnnd2*$^{-/-}$ mice ($p < 0.05$, (Fig. 7A, right panel)). TEM was further performed to assess differences in synaptic ultrastructure of hippocampal neurons (Fig. 7B, left panel). The number of synapse density in CA1 area was greatly reduced in mutant mice ($p < 0.05$, KO + Vector vs WT + Vector) that was further decreased by ShRictor ($p < 0.05$, KO + ShRictor vs KO + Vector; Fig. 7B, right panel). Furthermore, PSD thickness was remarkably reduced in the hippocampus of *Ctnnd2*$^{-/-}$ mice ($p < 0.05$, KO + Vector vs WT + Vector) that was also affected by shRNA-mediated Rictor knockdown ($p < 0.05$, KO + ShRictor vs KO + Vector) (Fig. 7C). Together, these data indicate that δ-catenin can regulate spine morphology and synaptic plasticity of neurons in brain, which is may contributed by Rictor-related signaling during synaptic development.

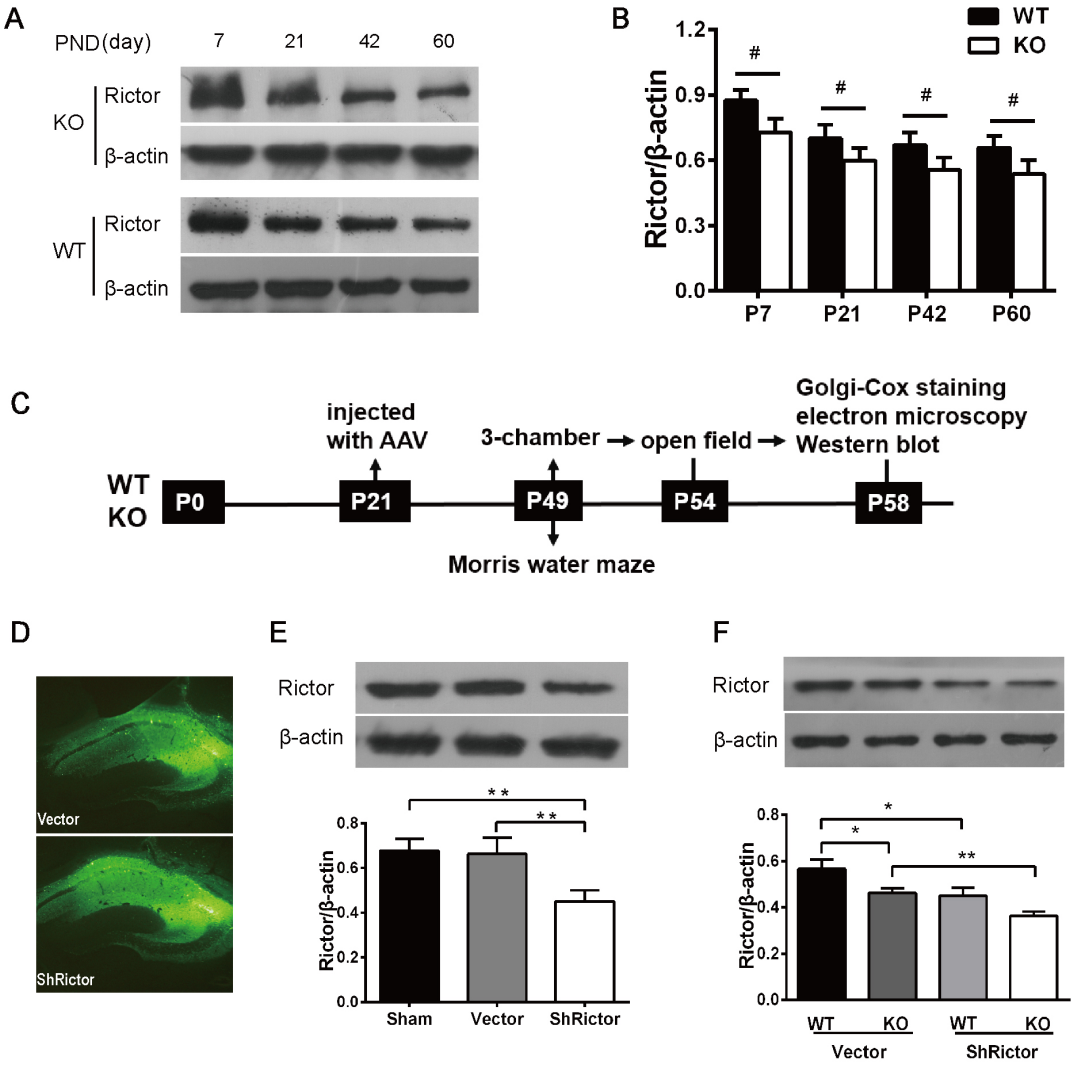

Fig. 3. Alteration of Rictor expression in *Ctnnd2*$^{-/-}$ mice. (A) Changes in hippocampal Rictor expression of mice at different developmental stages as indicated. (B) Quantification of Rictor expression in the hippocampus of *Ctnnd2*$^{-/-}$ mice and their control littermates. (C) The timeline of the WT. KO and/or ShRictor treatments and subsequent examinations. Treatments started from P21. Infections continued for 4 weeks until P49. Behavioral tests started from P49; n = 8 for only Morris water maze, n = 8 for 3-chamber and open field tests. The mice were then sacrificed at P58 for subsequent analyses, (D) Image of GFP expressed by the virus-carrying shRNA-Rictor construct were shown after infected the hippocampus of *Ctnnd2*$^{-/-}$ mice. (E, F) Verification of the efficiency of Rictor knockdown by Western blot in C57/BL6 mice (E) and the KO mice (F), respectively. Statistical analysis was performed using one-way ANOVA followed by a *post hoc* Tukey's test for multiple comparisons. n = 3–4 mice per group. Data are the means ± SEM.*, $p < 0.05$; **, $p < 0.01$; $^{\#}$, $p < 0.05$.

Furthermore, Western blot showed that the expression levels of postsynaptic proteins, such as ELKS and GluR1, were both markedly decreased in *Ctnnd2*$^{-/-}$ mice ($p < 0.05$, KO + Vector vs WT + Vector). ShRictor further deteriorated the reduction in expression levels of these two synaptic proteins ($p < 0.01$, KO + ShRictor vs KO + Vector) (Fig. 8A,B). In contrast, the expression of synapsin-1, a presynaptic marker protein, was neither changed by *Ctnnd2* mutation nor affected by ShRictor in mutant hippocampus (Fig. 6C). These results provide novel cues of synaptic basis for the pathogenesis of *Ctnnd2*$^{-/-}$ mice.

5. Discussion

In this study, we generated *Ctnnd2*-mutant mice with deletion of exon 2, and characterized their biochemical and behavioral phenotypes. These mutant mice exhibited autism-like behavioral phenotypes and defects in spatial cognition. The hippocampus of *Ctnnd2*$^{-/-}$ mice also showed significantly lower expression levels of Rictor protein and decreased actin dynamics. To our surprise, *in vivo* knockdown of Rictor by shRNA exacerbate the impairment of spatial learning and memory, but not autism-like behaviors. Mechanistically, we found that significant reduction in spine density, synapse number, and some synaptic

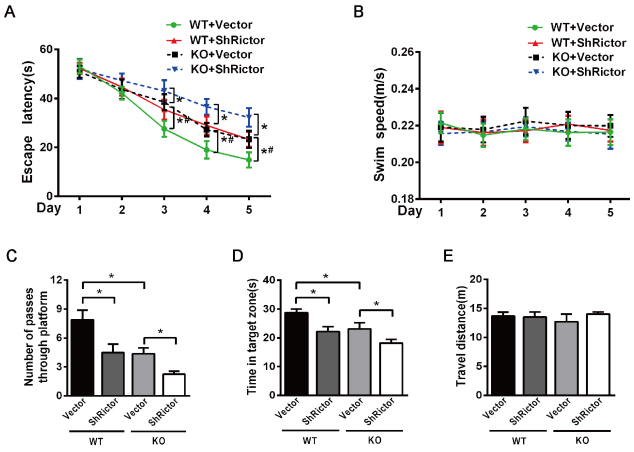

Fig. 4. Alteration of Rictor expression affects the spatial learning and memory in *Ctnnd2*$^{-/-}$ mice. (A–E) Morris water maze test of the mice. (A) Escape latency time to find the submerged platform and swim speed was observed from day 1 to day 5 of the learning phase (A, B). Statistical analysis was performed using two-way ANOVA followed by *post hoc* Tukey's test for multiple comparisons. (C–E) The number of platform crossing, time in the target zone, and travel distance were analyzed during the probe trial for spatial memory. n = 8 mice per group. Data are the means ± SEM. *, $p < 0.05$.

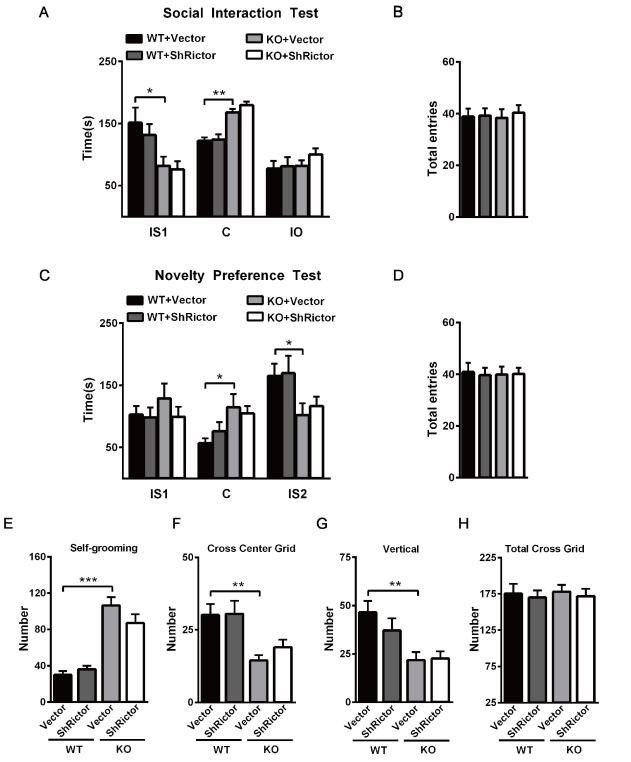

Fig. 5. No effects of Rictor knockdown on autism-like behavior of *Ctnnd2*$^{-/-}$ mice. (A–D) Social interaction and novelty preference were examined in the 3-chamber test. (E–H) Grooming times and numbers of center grid crossing, vertical rearing, climbing were measured in the open-field test in turn. Statistical analysis was performed using one-way ANOVA followed by a *post hoc* Tukey's test for multiple comparisons. n = 8 per group. Data are the means ± SEM. *, $p < 0.05$; **, $p < 0.01$; ***, $p < 0.001$.

protein expression within the hippocampus of *Ctnnd2*$^{-/-}$ mice. Our study provide a novel insight into the pivotal role of *CTNND2* gene in modulation of cognition via Rictor-mediated mTOR signaling and synaptic plasticity.

Based on previous studies, we have known that *CTNND2* is a candidate gene for intellectual disability and autism spectrum disorders, as intragenic deletion of this gene in patients could result in defects of brain cognition [2, 27] and autistic symptoms [3]. Thus, in our study, a mouse model with *CTNND2* gene mutation was generated and exhibited autism-like behavioral phenotypes, anxiety-like behavior with less exploration and deficits in spatial learning and memory. The CTNND2-mutant mice showed less exploration (as indicated by less vertical behaving) may largely due to deficits in cognition and (or) motivation but were without abnormal locomotion as the total number of crossed-grid in open field test (Fig. 1N; Fig. 5H) and total entries to distinct chambers in three-chamber sociability test (Fig. 1D,G; Fig. 5B,D) of CTNND2-KO mice was not significant difference with wild type mice. The swim speed of CTNND2-KO mice was also showed no difference when compared with those of WT mice (Figs. 2B,4B). These results demonstrate that the CTNND2-KO mouse model could to some extent mimic part of clinical features of these neurological diseases but without abnormal locomotor activity. Thus, it can be applied to study potential mechanisms of these disorders.

Recent evidence implicates synapses as important structural substrates for ASD pathogenesis [28]. The δ-catenin protein, which is encoded by *CTNND2* gene, is enriched in synaptosomes and is required for the regulation of spine and dendrite morphogenesis [5, 29]. Thus, loss function of δ-catenin is associated with deficits in synaptic transmission and dendrite extension via cadherin and PDZ-dependent interactions, especially in developmental stages [30]. Along with these lines, it is of great interest to observe the changes on actin polymerization, spine density, synapse density, and synaptic proteins levels in the hippocampus of *Ctnnd2*$^{-/-}$ mice and indeed multiple abnormalities were existed (Figs. 6,7,8), providing molecular and postsynaptic-structural basis for behavioral characteristics of the mutant mice.

As δ-catenin should interacting with Shank3 thus can target postsynaptic site [6]. Shank3 is an upstream node of PI3K/AKT signaling pathway which play pivotal role in mTOR signaling [7], and Rictor is a key regulatory and structural subunit of mTORC2 signaling that is required for AKT phosphorylation in multiple cells [31]. and is largely involved in learning and memory, we speculate that *CTNND2* gene would mediate autism-like behaviors and cognition deficits via mTOR2 signaling and Rictor would have great effects on modulation of these behavioral pheno-

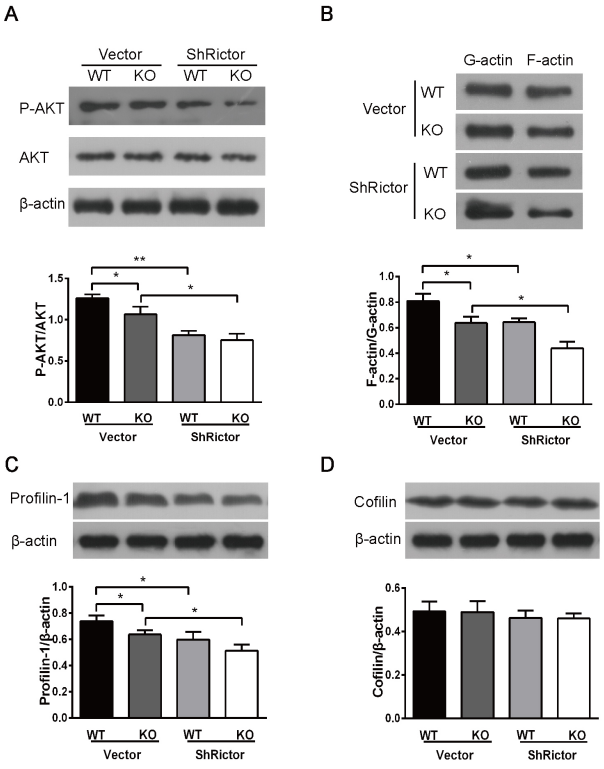

Fig. 6. Effects of Rictor knockdown on Akt phosphorylation and actin polymerization within the hippocampus of *Ctnnd2*$^{-/-}$ mice. (A) Expression levels of AKT and p-AKT (Ser473) were measured (upper panel) and analyzed (lower panel) by Western blot. (B) The ratio of F-actin/G-actin were analyzed by Western blot. (C, D) Expression levels of both Profilin-1 and Cofilin protein in each group were measured by Western blot, using WT and *Ctnnd2*$^{-/-}$ mice. Statistical analysis was performed using one-way ANOVA followed by *post hoc* Tukey's test for multiple comparisons. n = 3–4 mice per group. Data are the means ± SEM. *, $p < 0.05$; **, $p < 0.01$.

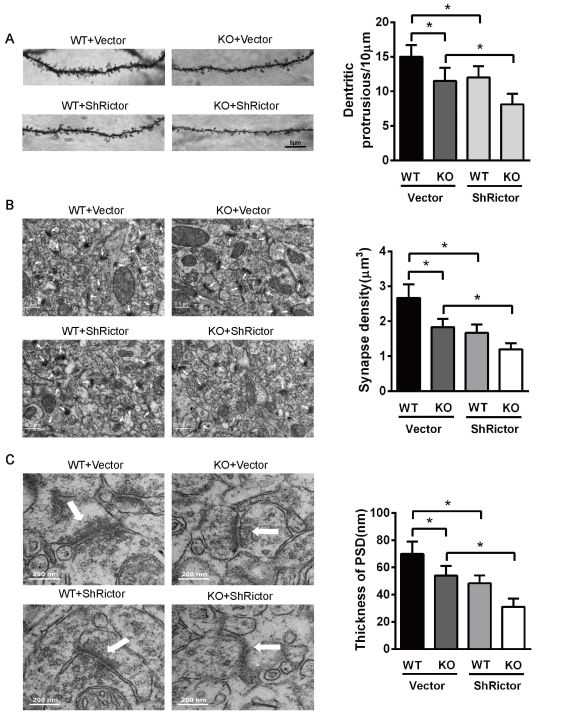

Fig. 7. Effects of Rictor knockdown on synaptic morphology of the mutant mice. (A) Spine density in hippocampal CA1 was assessed by Golgi-impregnation. Scale bar, 5 μm. (B, C) Synapse density (number of synapses *per* μm^3) and thickness of post-synaptic density (PSD) in hippocampal CA1 was determined by electron microscopy. Scale bars, 0.5 μm for B; 200 nm for C. Results was quantified as shown. Left, typical images; right, quantification of the results. Statistical analysis was performed using one-way ANOVA followed by *post hoc* Tukey's test for multiple comparisons. n = 3–4 mice per group. Data are the means ± SEM. *, $p < 0.05$.

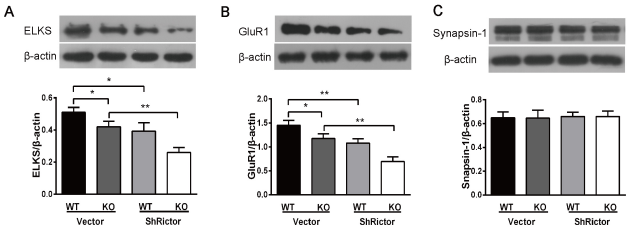

Fig. 8. Effects of Rictor on the expression of some typical synaptic proteins in the hippocampus of *Ctnnd2*$^{-/-}$ mice. Expression levels of the synaptic proteins ELKS (A), GluR1 (B), and Synapsin-1 (C) were measured by Western blot, respectively. Statistical analysis was performed using one-way ANOVA followed by *post hoc* Tukey's test for multiple comparisons. n = 3–4 mice per group. Data are the means ± SEM. *, $p < 0.05$; **, $p < 0.01$.

types. However, the exacerbation of learning and memory deficiency but not autism-like behaviors in both CTNND2-KO mice and WT mice with suppression of Rictor protein expression by shRNA. It is to some extent in line with other studies that conditionally knockdown or pharmacological suppression of Rictor would impair long-term memory and hippocampal long-term potentiation-dependent objective discrimination [12, 32], Other studies also shown that reduced mTORC2 activity in the hippocampus of Rictor fb-KO mice [11, 33], as mTORC2 is directly mediated with the phosphorylation at Ser-473 of Rictor downstream target AKT [34]. Both profilin-1 and cofilin are key regulators of actin dynamics [35, 36], and maintain F-actin/G-actin ratio in neurons that is required for the formation of dendritic spine and synapse development [37]. Actually, F-actin/G-actin ratio can be regulated by Rictor [32]. In our study, the reduction of profilin-1, F-actin/G-actin ratio were detected in *hippocampal neurons of Ctnnd2*$^{-/-}$ mice (Fig. 6C). These results may imply that *CTNND2*-gene mediated brain cognition mainly through Rictor-involved mTORC2/AKT signaling pathway. The mechanisms that *CTNND2* gene involved in regulating autism-like behaviors may be more complex and need further explore. Abnormal synaptic development and plasticity may represent a common pathogenesis for various human cognitive dys-

functions [38]. In our study, both synapse density and PSD thickness of hippocampal neurons were dramatically reduced in mutant mice which is in line with other studies [39, 40]. Despite the study reported that there were genes participating in the regulation of trans-synaptic signaling, primarily AMPA receptor signaling [4]. However, they did not prove the relationship between δ-catenin protein and the AMPA receptor GluR1 which is required for hippocampal LTP [41]. Furthermore, ELKS is a core component of the active zone within excitatory synapses [42]; both of these two postsynaptic proteins were significantly affected by *Ctnnd2* deletion or (and) Rictor knockdown (Fig. 8). These results provide structural changes at synaptic level that may contributed to the abnormal synaptic plasticity of hippocampal neurons in CTNND2-KO mice [43], underscoring Rictor-mediated function of δ-catenin in brain and the related neurological diseases.

6. Conclusions

In the study, we generated *Ctnnd2*$^{-/-}$ mice to investigate the role of this gene and potential mechanisms in certain neurological diseases. CTNND2-KO mice showed typical autism-like, anxiety-like behaviors, cognition deficiency and reduction of hippocampal Rictor protein. *CTNND2* gene participates in modulating spatial learning and memory but not autism-like behaviors mainly via Rictor-mediated mTORC2 signaling. Mechanistically, alters in actin dynamics and synaptic structures were existed in hippocampal neurons of this mutant mice. Our findings indicate that Rictor as a key regulator for the cytoskeletal dynamics underlying long-lasting structural plasticity and spatial cognition in *Ctnnd2*$^{-/-}$ mice.

7. Author contributions

SW supervised and organized the project. XW did major experiments, interpreted the data and wrote the manuscript. MX performed data curation. QX provide some resources. HT provide scientific advice. CS and FY help to writing and editing. LW contributed to data analysis. YW contributed to data collection and validation. JD help to behavioral experiments.

8. Ethics approval and consent to participate

Not applicable.

9. Acknowledgment

The authors gratefully acknowledge Professor Jiqiang Zhang of the Third Military Medical University for assistance with molecular biology experiments. The authors are grateful to all those who participated in this study.

10. Funding

This work was supported by the Science and Technology Project of Health Commission of Sichuan Province (No.18PJ430) and the Science and Technology Cooperation Project of Nanchong City and North Sichuan Medical College (20SXQT0077).

11. Conflict of interest

The authors declare no conflict of interest.

12. References

[1] Lu Q, Aguilar BJ, Li M, Jiang Y, Chen Y-H. Genetic alterations of δ-catenin/NPRAP/Neurojungin (*CTNND2*): functional implications in complex human diseases. Human Genetics. 2016; 135: 1107–1116.

[2] Hofmeister W, Nilsson D, Topa A, Anderlid B, Darki F, Matsson H, *et al*. *CTNND2*-a candidate gene for reading problems and mild intellectual disability. Journal of Medical Genetics. 2015; 52: 111–122.

[3] Turner TN, Sharma K, Oh EC, Liu YP, Collins RL, Sosa MX, *et al*. Loss of δ-catenin function in severe autism. Nature. 201; 520: 51–56.

[4] Reshetnikov VV, Kisaretova PE, Ershov NI, Shulyupova AS, Oshchepkov DY, Klimova NV, *et al*. Genes associated with cognitive performance in the Morris water maze: an RNA-seq study. Scientific Reports. 2020; 10: 22078.

[5] Arikkath J, Peng I, Ng YG, Israely I, Liu X, Ullian EM, *et al*. Delta-catenin regulates spine and synapse morphogenesis and function in hippocampal neurons during development. The Journal of Neuroscience. 2009; 29: 5435–5442.

[6] Hassani Nia F, Woike D, Martens V, Klüssendorf M, Hönck H, Harder S, *et al*. Targeting of δ-catenin to postsynaptic sites through interaction with the Shank3 N-terminus. Molecular Autism. 2020; 11: 85.

[7] Gropman AL. Epigenetics and Pervasive Developmental Disorders. In Epigenetics in Psychiatry (pp. 395–424). Academic Press. 2014.

[8] Chen C, Sgritta M, Mays J, Zhou H, Lucero R, Park J, *et al*. Therapeutic inhibition of mTORC2 rescues the behavioral and neurophysiological abnormalities associated with Pten-deficiency. Nature Medicine. 2019; 25: 1684–1690.

[9] Oh WJ, Jacinto E. mTOR complex 2 signaling and functions. Cell Cycle. 2011; 10: 2305–2316.

[10] Sarbassov DD, Ali SM, Kim D, Guertin DA, Latek RR, Erdjument-Bromage H, *et al*. Rictor, a novel binding partner of mTOR, defines a rapamycin-insensitive and raptor-independent pathway that regulates the cytoskeleton. Current Biology. 2004; 14: 1296–1302.

[11] Dadalko OI, Siuta M, Poe A, Erreger K, Matthies HJG, Niswender K, *et al*. mTORC2/rictor signaling disrupts dopamine-dependent behaviors via defects in striatal dopamine neurotransmission. The Journal of Neuroscience. 2015; 35: 8843–8854.

[12] Huang W, Zhu PJ, Zhang S, Zhou H, Stoica L, Galiano M, *et al*. MTORC2 controls actin polymerization required for consolidation of long-term memory. Nature Neuroscience. 2013; 16: 441–448.

[13] Urbanska M, Gozdz A, Swiech LJ, Jaworski J. Mammalian target of rapamycin complex 1 (mTORC1) and 2 (mTORC2) control the dendritic arbor morphology of hippocampal neurons. The Journal of Biological Chemistry. 2012; 287: 30240–30256.

[14] Lei W, Omotade OF, Myers KR, Zheng JQ. Actin cytoskeleton in dendritic spine development and plasticity. Current Opinion in Neurobiology. 2016; 39: 86–92.
[15] Johnson JL, Huang W, Roman G, Costa-Mattioli M. TORC2: a novel target for treating age-associated memory impairment. Scientific Reports. 2015; 5: 15193.
[16] Neves G, Cooke SF, Bliss TVP. Synaptic plasticity, memory and the hippocampus: a neural network approach to causality. Nature Reviews Neuroscience. 2008; 9: 65–75.
[17] Bailey CH, Kandel ER, Harris KM. Structural Components of Synaptic Plasticity and Memory Consolidation. Cold Spring Harbor Perspectives in Biology. 2015; 7: a021758.
[18] Woolfrey KM, Srivastava DP. Control of Dendritic Spine Morphological and Functional Plasticity by Small GTPases. Neural Plasticity. 2016; 2016: 3025948.
[19] Gilbert J, O'Connor M, Templet S, Moghaddam M, Di Via Ioschpe A, Sinclair A, *et al*. NEXMIF/KIDLIA Knock-out Mouse Demonstrates Autism-Like Behaviors, Memory Deficits, and Impairments in Synapse Formation and Function. The Journal of Neuroscience. 2020; 40: 237–254.
[20] Brigidi GS, Sun Y, Beccano-Kelly D, Pitman K, Mobasser M, Borgland SL, *et al*. Palmitoylation of δ-catenin by DHHC5 mediates activity-induced synapse plasticity. Nature Neuroscience. 2014; 17: 522–532.
[21] Chidambaram SB, Rathipriya AG, Bolla SR, Bhat A, Ray B, Mahalakshmi AM, *et al*. Dendritic spines: Revisiting the physiological role. Progress in Neuro-Psychopharmacology & Biological Psychiatry. 2019; 92: 161–193.
[22] Svitkina TM. Ultrastructure of the actin cytoskeleton. Current Opinion in Cell Biology. 2018; 54: 1–8.
[23] Laguesse S, Morisot N, Phamluong K, Sakhai SA, Ron D. MTORC2 in the dorsomedial striatum of mice contributes to alcohol-dependent F-Actin polymerization, structural modifications, and consumption. Neuropsychopharmacology. 2018; 43: 1539–1547.
[24] Thomanetz V, Angliker N, Cloëtta D, Lustenberger RM, Schweighauser M, Oliveri F, *et al*. Ablation of the mTORC2 component rictor in brain or Purkinje cells affects size and neuron morphology. Journal of Cell Biology. 2013; 201: 293–308.
[25] Desmond NL, Levy WB. Changes in the numerical density of synaptic contacts with long-term potentiation in the hippocampal dentate gyrus. The Journal of Comparative Neurology. 1986; 253: 466–475.
[26] Zhao Y, He L, Zhang Y, Zhao J, Liu Z, Xing F, *et al*. Estrogen receptor alpha and beta regulate actin polymerization and spatial memory through an SRC-1/mTORC2-dependent pathway in the hippocampus of female mice. The Journal of Steroid Biochemistry and Molecular Biology. 2017; 174: 96–113.
[27] Belcaro C, Dipresa S, Morini G, Pecile V, Skabar A, Fabretto A. *CTNND2* deletion and intellectual disability. Gene. 2015; 565: 146–149.
[28] Joensuu M, Lanoue V, Hotulainen P. Dendritic spine actin cytoskeleton in autism spectrum disorder. Progress in Neuro-Psychopharmacology & Biological Psychiatry. 2018; 84: 362–381.
[29] Yuan L, Seong E, Beuscher JL, Arikkath J. Δ-Catenin Regulates Spine Architecture via Cadherin and PDZ-dependent Interactions. The Journal of Biological Chemistry. 2015; 290: 10947–10957.
[30] Baumert R, Ji H, Paulucci-Holthauzen A, Wolfe A, Sagum C, Hodgson L, *et al*. Novel phospho-switch function of delta-catenin in dendrite development. Journal of Cell Biology. 2020; 219: e201909166.
[31] Zheng B, Wang J, Tang L, Tan C, Zhao Z, Xiao Y, *et al*. Involvement of Rictor/mTORC2 in cardiomyocyte differentiation of mouse embryonic stem cells in vitro. International Journal of Biological Sciences. 2017; 13: 110–121.
[32] Zhao J, Bian C, Liu M, Zhao Y, Sun T, Xing F, *et al*. Orchiectomy and letrozole differentially regulate synaptic plasticity and spatial memory in a manner that is mediated by SRC-1 in the hippocampus of male mice. The Journal of Steroid Biochemistry and Molecular Biology. 2019; 178: 354–368.
[33] Zhu PJ, Chen C, Mays J, Stoica L, Costa-Mattioli M. mTORC2, but not mTORC1, is required for hippocampal mGluR-LTD and associated behaviors. Nature Neuroscience. 2018; 21: 799–802.
[34] Laplante M, Sabatini DM. MTOR signaling in growth control and disease. Cell. 2012; 149: 274–293.
[35] Funk J, Merino F, Venkova L, Heydenreich L, Kierfeld J, Vargas P, *et al*. Profilin and formin constitute a pacemaker system for robust actin filament growth. Elife. 2019; 8: e50963.
[36] McCall PM, MacKintosh FC, Kovar DR, Gardel ML. Cofilin drives rapid turnover and fluidization of entangled F-actin. Proceedings of the National Academy of Sciences. 2019; 116: 12629–12637.
[37] Ackermann M, Matus A. Activity-induced targeting of profilin and stabilization of dendritic spine morphology. Nature Neuroscience. 2003; 6: 1194–1200.
[38] Volk L, Chiu S, Sharma K, Huganir RL. Glutamate synapses in human cognitive disorders. Annual Review of Neuroscience. 2015; 38: 127–149.
[39] Buffington SA, Huang W, Costa-Mattioli M. Translational control in synaptic plasticity and cognitive dysfunction. Annual Review of Neuroscience. 2014; 37: 17–38.
[40] Modi B, Pimpinella D, Pazienti A, Zacchi P, Cherubini E, Griguoli M. Possible Implication of the CA2 Hippocampal Circuit in Social Cognition Deficits Observed in the Neuroligin 3 Knock-out Mouse, a Non-Syndromic Animal Model of Autism. Frontiers in Psychiatry. 2019; 10: 513.
[41] Edfawy M, Guedes JR, Pereira MI, Laranjo M, Carvalho MJ, Gao X, *et al*. Abnormal mGluR-mediated synaptic plasticity and autism-like behaviours in Gprasp2 mutant mice. Nature Communications. 2019; 10: 1431.
[42] Südhof TC. The presynaptic active zone. Neuron. 2012; 75: 11–25.
[43] Sheng M, Hoogenraad CC. The Postsynaptic Architecture of Excitatory Synapses: a more Quantitative View. Annual Review of Biochemistry. 2007; 76: 823–847.

Abbreviations: ASD, Autism spectrum disorder; PSD, postsynaptic density; GluR1, glutamate receptor 1; PND, postnatal day; AAV, adeno-associated virus; LTP, long-term potentiation.

Keywords: *CTNND2* gene; Autism; mTOR signaling; Rictor; Learning and memory

Send correspondence to: Shali Wang, Cerebrovascular Disease Laboratory, Institute of Neuroscience, Chongqing Medical University, 400016 Chongqing, China, Department of Physiology, School of Basic Medical Sciences, Chongqing Medical University, 400016 Chongqing, China, E-mail: 100472@cqmu.edu.cn